JAERI-M
7309

LOSS MECHANISM OF THE SUPERTHERMAL ELECTRONS ACROSS THE SEPARATRIX INTO THE SCRAPE-OFF LAYER IN DIVA

October 1977

S. YAMAMOTO, S. SENGOKU, H. KIMURA,
Y. SHIMOMURA, H. MAEDA, H. OHTSUKA,
K. ODAJIMA, M. NAGAMI, N. UEDA*

日本原子力研究所
Japan Atomic Energy Research Institute

この報告書は，日本原子力研究所が JAERI-M レポートとして，不定期に刊行している研究報告書です．入手，複製などのお問合わせは，日本原子力研究所技術情報部（茨城県那珂郡東海村）あて，お申しこしください．

JAERI-M reports, issued irregularly, describe the results of research works carried out in JAERI. Inquiries about the availability of reports and their reproduction should be addressed to Division of Technical Information, Japan Atomic Energy Research Institute, Tokai-mura, Naka-gun, Ibaraki-ken, Japan.

JAERI-M 7309

Loss Mechanism of the Superthermal Electrons Across the Separatrix into the Scrape-Off Layer in DIVA

Shin YAMAMOTO, Seio SENGOKU, Haruyuki KIMURA, Yasuo SHIMOMURA
Hikosuke MAEDA, Hideo OHTSUKA, Kazuo ODAJIMA, Masayuki NAGAMI
and Noriaki UEDA*

Division of Thermonuclear Fusion Research,
Tokai Research Establishment, JAERI

(Received September 2, 1977)

Behavior of superthermal electrons is investigated by using X-ray measurement and electrostatic energy analyser. Superthermal electrons are divided into two groups; i.e. high energy electrons (10 keV - 100 keV) and epithermal electrons (150 eV - 500 eV). Loss flux of the epithermal electrons is obtained and their loss is shown to be explained by destruction of magnetic surfaces near the separatrix due to non-axisymmetric perturbations. Two-dimensional path of high energy electrons is obtained and the effects of non-axisymmetric perturbations on the drift surface are described.

Keywords: Superthermal Electron, Scrape-Off Layer, Divertor, Separatrix, Non-Axisymmetric Perturbation, DIVA Tokamak, Electron Loss, 10 keV - 100 keV Range, 150 eV - 500 eV Range

---

* On leave from Mitsubishi Atomic Power Ind., Ohmiya, Japan

JAERI－M　7309

DIVAにおける高速電子のセパラトリックスを横切り，スクレイプ・オフ層に損失する機構

日本原子力研究所核融合研究部

山本　　新・仙石　盛夫・木村　晴行
下村　安夫・前田　彦祐・大塚　英男
小田島和男・永見　正幸・上田　憲照*

（1977年 9月 2日受理）

DIVAにおいて高速電子のふるまいを，X－線および静電エネルギーアナライザーによって調べた。スクレイプ・オフ層において観察される高速電子は2つの組に分けられる。すなわち，10 keV － 100 keV程度のエネルギーを持った電子および150 eV － 500 eV程度の電子である。150 eV － 500 eV程度の電子は定量的に調べられ，それらの損失は非軸対称磁場によるセパラトリックス近傍での磁気面の破壊により説明できることが明かとなった。10 keV － 100 keV 程度の電子の二次元的軌道が得られた。非軸対称磁場による擾乱の，それらの粒子への影響についての議論をおこなった。

＊　外来研究員　三菱原子力工業株式会社

CONTENTS

1. Introduction

Several distinct runaway regimes in tokamaks are identified depending on the extent to which runaways are present, their energy, and confinement quality. These are categorized as a weak, continuous, and strong runaway regimes. The presence of each regime has been well-documented in various tokamak devices [1-3]. The weak runaway regime is present during a normal, stable tokamak discharge and is characterized by a very low density of runaways.

In this paper, superthermal electrons are studied in a weak runaway regime in DIVA with an axisymmetric divertor. The superthermal electrons in this paper are divided into two groups, that is, high energy electrons (10 keV - 100 keV) and epithermal electrons (150 eV - 500 eV). An X-ray probe is used to search for the path of high energy electrons. A Faraday cup (multi-grid energy analyzer) is used for the measurement of the energy spectrum and flux of the epithermal electrons. By operating a divertor, these probes in the scrape-off layer can be used without disturbing the main plasma for studying superthermal electrons.

Superthermal electrons provide a sensitive means probing field perturbations, which affect not only on a plasma confinement but also the scrape-off layer. Especially the epithermal electrons in the scrape-off layer affect the heat flux to the divertor [13-15]. These electrons may be continuously generated and lost throughout the discharge. A model is presented to explain the loss mechanism of the epithermal electrons across the separatrix. This model describes a destruction of magnetic surfaces near the separatrix due to the non-axisymmetric perturbations, and may account for the amounts of the lower energy epithermal electrons in the scrape-off layer in the divertor region.

The high energy electrons are observed only in low density plasmas and/or in high loop-voltage plasmas. The measured drift surface of high energy electrons may be also explained by the model.

Experimental apparatus and operating conditions are given in Section 2. Experimental results for the epithermal electrons are described in Section 3. A model for the loss mechanism of the epithermal electrons is presented in Section 4. The study on high energy electrons is given in Section 5 and conclusions are in Section 6.

2. Experimental Apparatus and Operating Conditions

Detailed description of DIVA was reported in Refs. [4, 5]. A schematic diagram of the layout used for the experiments is given in Fig. 1.

Plasma equilibrium with a separatrix magnetic surface is obtained in a shell with an opening towards a divertor hoop.

A Faraday cup (multi-grid energy analyzer) is used for the measurements of the energy spectrum and particle flux of the epithermal electrons (150 eV - 500 eV). Detailed description of this probe is given in Ref. [6]. Targets are used for searching the path of high energy electrons (10 keV - 100 keV) in the scrape-off layer. The target supported by a stainless steel pipe (2 mm in diameter) is a molybdenum tip of cylindrical shape and its axis is parallel to the toroidal magnetic field. One side of the cylinder is cut off under the angle 45° and its surface is the source of X-ray radiation which we observe. Namely the target is oriented so that the high energy electrons from the main plasma can hit the observed surface. The collimation is so made that the X-ray beams from that surface can pass to the scintillator and the light from the scintillator is transmitted to the photomultiplier, using fiber light guides.

One X-ray probe with target (a) is used to study a two-dimensional structure of the drift surface of the high energy electrons. This target (4 mm in diameter) is mechanically to be located at any position in the scrape-off layer. X-ray from the surface of the target (a) is measured through a quartz glass (8 mm in thickness).

The other X-ray probe (see Fig. 2) with a smaller target (b) (1 mm in diameter) is used to study the spread of the path of the high energy electrons at R = 40 cm in the divertor region. The whole assembly of the target (b), scintillator, and the collimator is vertically movable so that the target can be placed at any position between Z = 0 and Z = 6 cm without changing the solid angle of observation. X-ray energy which we observe with 100% efficiency range from approximately 10 keV to 100 keV is determined by the thickness of an aluminum window and the height of the NaI(Tl) scintillator.

The experiments were mainly performed under the following conditions. The movable shell is at the open position, protection plates extend 5 mm from the shell, and no titanium is flushed. Toroidal magnetic field is fixed at 1T and hydrogen gas of 1.5×10^{18} atoms is admitted by four fast acting valves. Additional hydrogen gas of 3.4×10^{19} atoms/sec is injected

during the discharge. Plasma current $I_p \simeq 14$ kA and divertor hoop current $I_D \simeq 1.2 \times I_p$. Figure 3 shows a typical time evolution of the main plasma parameters, including I_p, loop voltage V_L, total number of electrons N_e and hard X-ray radiation. The electron temperature T_e at R = 62 cm and Z = -1 cm near the center measured by Thomson scattering is about 250 eV, and the ion temperature is 85 eV from the neutral particle energy analysis. The electron temperature and the density in the scrape-off layer measured by Langmuir probes and the Faraday cup are 40 eV and 1×10^{12} cm^{-3} at t = 10 msec, respectively.

Typical plasma parameter are tabulated in Table I.

3. Epithermal Electrons in the Scrape-off Layer

Figure 4 shows vertical profile and time evolution of particle flux of the epithermal electrons measured with the Faraday cup at R = 40 cm. Open circles denote the particle fluxes in the energy above 150 eV, and closed circles denote those in the energy above 300 eV. The epithermal electrons in the energy from 150 eV to 300 eV, are observed in the scrape-off layer throughout the discharge. The total electron current to the divertor due to the epithermal electrons is about 1A at 10 msec, while ion saturation current is about 20A.

Figures 5-(a) and -(b) show the energy spectrum of the epithermal electrons measured at R = 40 cm and Z = ±4.5 cm. The epithermal electrons (150 eV - 500 eV) exist not only on the upper side to the equatorial plane but also on the lower side. However, the amount on the lower side is very small and their energy is low. Mean free path of the epithermal electrons in the scrape-off layer in DIVA is several hundred meters and is much greater than the connection length from the main plasma to the divertor, which is about 10 m. Once the epithermal electrons flow into the scrape-off layer from the main plasma, they go to the divertor plate through the scrape-off layer without collisions and disappear after colliding with the divertor plate (See Fig. 1). These results indicate that the epithermal electrons must be continuously generated due to the acceleration of the toroidal electric field in the vicinity of the main plasma and lost across the separatrix throughout the discharge. The energy spectrum of the epithermal electrons shows that the confinement time of these electrons in the main plasma is very short compared with the deflection time.

We can estimate the velocity of these electrons across the magnetic

during the discharge. Plasma current $I_p \simeq 14$ kA and divertor hoop current $I_D \simeq 1.2 \times I_p$. Figure 3 shows a typical time evolution of the main plasma parameters, including I_p, loop voltage V_L, total number of electrons N_e and hard X-ray radiation. The electron temperature T_e at R = 62 cm and Z = -1 cm near the center measured by Thomson scattering is about 250 eV, and the ion temperature is 85 eV from the neutral particle energy analysis. The electron temperature and the density in the scrape-off layer measured by Langmuir probes and the Faraday cup are 40 eV and 1×10^{12} cm^{-3} at t = 10 msec, respectively.

Typical plasma parameter are tabulated in Table I.

3. Epithermal Electrons in the Scrape-off Layer

Figure 4 shows vertical profile and time evolution of particle flux of the epithermal electrons measured with the Faraday cup at R = 40 cm. Open circles denote the particle fluxes in the energy above 150 eV, and closed circles denote those in the energy above 300 eV. The epithermal electrons in the energy from 150 eV to 300 eV, are observed in the scrape-off layer throughout the discharge. The total electron current to the divertor due to the epithermal electrons is about 1A at 10 msec, while ion saturation current is about 20A.

Figures 5-(a) and -(b) show the energy spectrum of the epithermal electrons measured at R = 40 cm and Z = ±4.5 cm. The epithermal electrons (150 eV - 500 eV) exist not only on the upper side to the equatorial plane but also on the lower side. However, the amount on the lower side is very small and their energy is low. Mean free path of the epithermal electrons in the scrape-off layer in DIVA is several hundred meters and is much greater than the connection length from the main plasma to the divertor, which is about 10 m. Once the epithermal electrons flow into the scrape-off layer from the main plasma, they go to the divertor plate through the scrape-off layer without collisions and disappear after colliding with the divertor plate (See Fig. 1). These results indicate that the epithermal electrons must be continuously generated due to the acceleration of the toroidal electric field in the vicinity of the main plasma and lost across the separatrix throughout the discharge. The energy spectrum of the epithermal electrons shows that the confinement time of these electrons in the main plasma is very short compared with the deflection time.

We can estimate the velocity of these electrons across the magnetic

field, using the rate of runaway production and the loss rate experimentally obtained. In the stationary state, total current I of these electrons in the scrape-off layer is given by,

$$I \simeq S \cdot d \cdot q \cdot 2\pi R \cdot 2\pi a \tag{3-1}$$

where S is the rate of runaway production, d is the width of a domain where these electrons are produced, q is the charge of the particle and R and a are the major and minor radii.

The rate of runaway production has been given by Lebedev [7] as,

$$S = 2^{1/3}\pi^{-1/2}N\nu\alpha^{-1/2}\exp(-1/2\alpha^2-2/\alpha-1/2) \tag{3-2}$$

where $\alpha^2 = ET/2\pi e^3 N\Lambda$

N = electron density which is equal to the ion density

T = electron temperature

ν = electron-electron collision frequency for thermal velocities

$= 4\pi e^4 N\Lambda/\sqrt{mT^3}$

Λ = Coulomb logarithm

and E = electric field

Taking the experimental values at the edge of the main plasma at t = 10 msec in DIVA,

$$V_L = 2\pi RE = 4 \text{ V}, \quad T = 40 \text{ eV} \quad \text{and} \quad N = 1 \times 10^{12} \text{ cm}^{-3}$$

we obtain, for the rate of runaway production in the vicinity of main plasma:

$$S \sim 1 \times 10^{15} \text{ cm}^{-3}\text{sec}^{-1}$$

If we substitute the above production rate and other DIVA data into Eq. (3-1), where $I \sim 1$A, $S \sim 1 \times 10^{15}$ cm$^{-3}\cdot$sec^{-1}, $q = 1.6 \times 10^{-19}$ coulomb, $R \sim 60$ cm and $a \sim 10$ cm, the equation gives

$$d \sim 3 \times 10^{-1} \text{ [cm]} \tag{3-3}$$

If these electrons are freely accelerated by the toroidal electric field until diverted, the necessary time for these electrons to reach the

average energy of 200 eV is about

$$t \sim 30 \times 10^{-6} \text{ [sec]} , \tag{3-4}$$

and the circulation number of these electrons around the torus until diverted is about 50 in the present plasma parameter. Using the results (3-3) and (3-4), the velocity of these electrons across the magnetic field is obtained as follows.

$$V_r = d/t$$
$$= 9 \times 10^3 \text{ [cm/sec]}$$

Thus, the equivalent diffusion coefficient of these electrons are estimated as follows,

$$D \sim d \cdot V_r$$
$$\sim 3 \times 10^3 \text{ [cm}^2\text{/sec]} .$$

The above diffusion coefficient of the epithermal electrons is greater than that of particles in the divertor region at $R \simeq 40$ cm, as estimated from the vertical profiles of ion saturation currents at different major radii [4]. These results suggest that observed large diffusion coefficient is not explained by Coulomb scattering, and has to be explained by other mechanisms.

4. Model for Loss Mechanism of Lower Energy Epithermal Electrons

The observed very large loss rate of the epithermal electrons seems to be due to free motion of these electrons along ergodic magnetic surfaces. It is well known that sub-harmonic resonances in the rotational transform lead to bands of islands which become more pronounced as the separatrix is approached, and that near the separatrix there appear to be no stable magnetic surfaces [8-11]. The drift surface of the epithermal electrons nearly coincides with the magnetic surface. Thus the non-axisymmetric perturbations have a possibility to explain the observed large loss rate of the epithermal electrons.

In order to clarify the effect of the non-axisymmetric perturbations on DIVA configuration, we calculate numerically the width of the ergodic region near the old separatrix and the circulation number of field lines around the torus until diverted under the effect of the perturbations.

average energy of 200 eV is about

$$t \sim 30 \times 10^{-6} \text{ [sec]} , \tag{3-4}$$

and the circulation number of these electrons around the torus until diverted is about 50 in the present plasma parameter. Using the results (3-3) and (3-4), the velocity of these electrons across the magnetic field is obtained as follows.

$$V_r = d/t$$
$$= 9 \times 10^3 \text{ [cm/sec]}$$

Thus, the equivalent diffusion coefficient of these electrons are estimated as follows,

$$D \sim d \cdot V_r$$
$$\sim 3 \times 10^3 \text{ [cm}^2\text{/sec]} .$$

The above diffusion coefficient of the epithermal electrons is greater than that of particles in the divertor region at $R \simeq 40$ cm, as estimated from the vertical profiles of ion saturation currents at different major radii [4]. These results suggest that observed large diffusion coefficient is not explained by Coulomb scattering, and has to be explained by other mechanisms.

4. Model for Loss Mechanism of Lower Energy Epithermal Electrons

The observed very large loss rate of the epithermal electrons seems to be due to free motion of these electrons along ergodic magnetic surfaces. It is well known that sub-harmonic resonances in the rotational transform lead to bands of islands which become more pronounced as the separatrix is approached, and that near the separatrix there appear to be no stable magnetic surfaces [8-11]. The drift surface of the epithermal electrons nearly coincides with the magnetic surface. Thus the non-axisymmetric perturbations have a possibility to explain the observed large loss rate of the epithermal electrons.

In order to clarify the effect of the non-axisymmetric perturbations on DIVA configuration, we calculate numerically the width of the ergodic region near the old separatrix and the circulation number of field lines around the torus until diverted under the effect of the perturbations.

To represent the basic feature of the unperturbed configuration in DIVA, a model is used, consisting of two filamentary circular rings located at the center of the main plasma (R_p = 0.61 m) with current I_p, and at the divertor hoop position (R_D = 0.37 m) with current I_D. And also shaping coils are used, which make magnetic surfaces fit the shell surface. This model well describes the magnetic configurations near the separatrix in the equilibrium [12]. We use the (R, Φ, Z) co-ordinate system to describe toroidal magnetic surfaces and field lines (Fig. 6).

The invariant surfaces form a family of nested closed surfaces, as illustrated in Fig. 7, which surround the plasma circular ring, are axisymmetric. This family of closed surface is bounded by a separatrix surface beyond which the surface are extended to the divertor region. The location of the separatrix magnetic surface is determined by the ratio of the divertor hoop current I_D to the plasma current I_p. Perturbations of field lines destroy the axial symmetry and the absolute existance of surface. In this section, we consider a perturbation described by the following relations.

$$\tilde{B}_R = -\alpha \, \mathrm{SIN}(N\Phi)$$

$$\tilde{B}_Z = -\frac{\alpha Z}{R} \, \mathrm{SIN}(N\Phi)$$

where α is the strength of the perturbation and N is the toroidal number of perturbation. These expressions satisfy the relation div $\vec{B}$ = 0 and simulate the perturbation arising from a setting error of the toroidal coils to the meridian plane. The fourth order R.K.G. method is applied to investigate the equations describing the field lines.

$$\frac{dR}{B_R^{(0)} + \tilde{B}_R} = \frac{Rd\Phi}{B_\Phi} = \frac{dZ}{B_Z^{(0)} + \tilde{B}_Z}$$

The field lines are traced back by the same method from the final point to the initial start point (R_0, Φ_0, Z_0) to check the numerical errors. The accuracy of the calculations is 10^{-9}.

Numerical calculations are made for a range of DIVA, that is, the ratio of the divertor current I_D (I_D = -16 kA) to the plasma current I_p (I_p = -13.3 kA) is 1.2 and the toroidal magnetic field is 1T. The positions of the shaping coils are R = 110 cm and Z = ±70 cm and the current I_S is 8 kA. Figure 7 gives a typical set of field surfaces. The position of the null point of the separatrix is in the region between R = 46.18 cm and R = 46.19 cm on the equatorial plane.

Figure 8 shows the behaviors of the field lines near the old separatrix in the case of $\alpha = 10^{-3}$ T and N = 1. The field lines are followed for 70 turns around the torus in the counter direction to the plasma current. This direction corresponds to that of acceleration of electrons by the toroidal electric fields. The dots in the figure denote the co-ordinate of the point depicting the field line through each field period with initial values $R_0 = 46.46$ cm, $Z_0 = 0$ cm and $\Phi_0 = 0$. The field lines through the initial point are diverted after 42 circuits around the torus. The region A in Fig. 8 is expanded in Fig. 9. The solid lines show the old separatrix. We find the islands at an old q = 10 rational surface and small isolated islands at an old q = 11 rational surface. Table II gives numerical results of the circulation number of field lines around the torus until diverted, which start out at various points on the equatorial plane in the ergodic region.

These results show that the width of the ergoidc region is at least several mm, in which the circulation number of field lines around the torus until diverted is about 50 in the case $\alpha = 10^{-3}$ T and N = 1. Thus, a field error of $\alpha = 10^{-3}$ T can explain the loss of the epithermal electrons and the quantity of these electrons in the scrape-off layer in the divertor region, which were discussed in the previous section. Figure 8 and 9 also show that non-axisymmetric perturbations spread the magnetic surface near the old separatrix in the divertor region.

The case of $\alpha = 10^{-3}$ T and N = 1 corresponds to the case in which the angle of the toroidal coil to the meridian plane is about 0.1°.

5. Effects of Non-Axisymmetric Perturbations on High Energy Electrons

In the preceding section, we have shown that non-axisymmetric perturbations spread the magnetic surfaces near the old separatrix in the divertor region. In this section, we discuss the effects of non-axisymmetric perturbations on the drift surface of high energy electrons. X-ray target probe with a small target (b) (1 mm in diameter) is used to study the spread of the path of the high energy electrons.

Figure 10 shows the path of high energy electrons at t = 20 msec in the later phase of the discharge where the plasma density is low. The path is obtained, using the target (a) (4 mm in diameter) shown in Fig. 1. The closed circles, inside the shell, show the first detectable positions when the target (a) is scanned vertically on each plane. Figure 10 clearly shows

Figure 8 shows the behaviors of the field lines near the old separatrix in the case of $\alpha = 10^{-3}$ T and N = 1. The field lines are followed for 70 turns around the torus in the counter direction to the plasma current. This direction corresponds to that of acceleration of electrons by the toroidal electric fields. The dots in the figure denote the co-ordinate of the point depicting the field line through each field period with initial values $R_0 = 46.46$ cm, $Z_0 = 0$ cm and $\Phi_0 = 0$. The field lines through the initial point are diverted after 42 circuits around the torus. The region A in Fig. 8 is expanded in Fig. 9. The solid lines show the old separatrix. We find the islands at an old q = 10 rational surface and small isolated islands at an old q = 11 rational surface. Table II gives numerical results of the circulation number of field lines around the torus until diverted, which start out at various points on the equatorial plane in the ergodic region.

These results show that the width of the ergoidc region is at least several mm, in which the circulation number of field lines around the torus until diverted is about 50 in the case $\alpha = 10^{-3}$ T and N = 1. Thus, a field error of $\alpha = 10^{-3}$ T can explain the loss of the epithermal electrons and the quantity of these electrons in the scrape-off layer in the divertor region, which were discussed in the previous section. Figure 8 and 9 also show that non-axisymmetric perturbations spread the magnetic surface near the old separatrix in the divertor region.

The case of $\alpha = 10^{-3}$ T and N = 1 corresponds to the case in which the angle of the toroidal coil to the meridian plane is about 0.1°.

5. Effects of Non-Axisymmetric Perturbations on High Energy Electrons

In the preceding section, we have shown that non-axisymmetric perturbations spread the magnetic surfaces near the old separatrix in the divertor region. In this section, we discuss the effects of non-axisymmetric perturbations on the drift surface of high energy electrons. X-ray target probe with a small target (b) (1 mm in diameter) is used to study the spread of the path of the high energy electrons.

Figure 10 shows the path of high energy electrons at t = 20 msec in the later phase of the discharge where the plasma density is low. The path is obtained, using the target (a) (4 mm in diameter) shown in Fig. 1. The closed circles, inside the shell, show the first detectable positions when the target (a) is scanned vertically on each plane. Figure 10 clearly shows

that high energy electrons are well-guided along the diverted magnetic field lines to the divertor under the acceleration of the toroidal electric field. Figure 11 shows vertical profiles of X-ray intensities from the target and particle fluxes of the epithermal electrons in the energy above 150 eV, on three planes (R = 40, 43 and 45 cm) and t = 20 msec. The position at R = 45 cm is near the null point but outside the main plasma. It should be noted that not only epithermal electrons but also high energy electrons widly exist along the vertical axis in the divertor region.

In order to increase the spatial resolutions, we use X-ray probe with a small target (b) (1 mm in diameter) at R = 40 cm. Figure 12 shows the vertical profiles and time evolution of high energy electrons measured by the target probe. The results show that the full half width of the high energy electrons is 1 cm.

Particle orbits of high energy electrons in the axisymmetric magnetic fields [see Section 4] are numerically calculated, using the guiding center approximation. The toroidal electric field is not considered. Figure 13 shows the numerical results of drift surfaces of high energy electrons in DIVA, projected on a minor cross section. The solid lines denote the electrons in the energy of 100 keV and the broken line in the energy of 10 keV. The dotted line denotes the separatrix. The high energy electrons with the energy of 100 keV, which start out at the point R = 71.02 cm at the right hand side on the equatorial plane, are confined, while the electrons, which start out at R = 71.03 cm are lost to the divertor. The results show that the critical drift surface from which the 100 keV electrons are diverted, intersects the region between R = 71.02 cm and R = 71.03 cm. Table III gives the numerical results of the region where the critical drift surfaces of high energy electrons in the energy of 100 keV and 10 keV, and also the separatrix surface exist at right hand side on the equatorial plane.

These results show the difference between the trajectory of diverted high energy electrons in the energy of 100 keV and that of 10 keV is about 10 mm at the right hand side on the equatorial plane, but the difference of that in the divertor region between R = 40 cm and R = 46 cm is within 3 mm. These numerical results show the energy difference of these electrons cannot explain the observed spread of the high energy electrons shown in Figs. 11 and 12.

Another possibility to explain the spread of the drift surface in the divertor region is the movement (or fluctuation) of the equilibrium position.

The observed width of the movement of the null points is less than 3 mm, which gives only 1.5 mm spread at R = 40 cm. Thus this mechanism seems no to be influential on the spread of the drift surfaces.

The non-axisymmetric perturbations may explain the spread of the path of high energy electrons.

6. Conclusions

Behaviors of superthermal electrons in the scrape-off layer in DIVA are experimentally studied. Superthermal electrons are divided into two groups, that is, high energy electrons (10 keV - 100 keV) and epithermal electrons (150 eV - 500 eV). In the normal discharge, the epithermal electrons play an important role in the heat flux density in the scrape-off layer [13-15]. The loss flux of these electrons is measured and explained by a model assuming the destruction of the magnetic surface near the separatrix due to non-axisymmetric perturbations. The observed spread of the path of high energy electrons also may be explained by the model.

It is necessary to control the density of the superthermal electrons in the scrape-off layer to reduce heavy impurity contamination caused by the evaporation.

The spread of the flux surfaces near the old separatrix due to non-axisymmetric perturbations has a possibility of a reduction of heat flux density on the neutralizer plate or limiter.

Acknowledgments

Our particular thanks are due to Drs. S. Seki, S. Matsuda, M. Yoshikawa, M. Tanaka and Y. Tanaka for their fruitful discussions. We would like to thank Dr. T. Funahashi, Dr. T. Yamauchi and Mr. K. Kumagai for the electron temperature measurement. We are also grateful to Drs. Y. Obata and S. Mori for their continuous encouragement of our work. The members of operating group of DIVA are gratefully acknowledged for their assistance in the experiment.

The observed width of the movement of the null points is less than 3 mm, which gives only 1.5 mm spread at R = 40 cm. Thus this mechanism seems no to be influential on the spread of the drift surfaces.

The non-axisymmetric perturbations may explain the spread of the path of high energy electrons.

6. Conclusions

Behaviors of superthermal electrons in the scrape-off layer in DIVA are experimentally studied. Superthermal electrons are divided into two groups, that is, high energy electrons (10 keV - 100 keV) and epithermal electrons (150 eV - 500 eV). In the normal discharge, the epithermal electrons play an important role in the heat flux density in the scrape-off layer [13-15]. The loss flux of these electrons is measured and explained by a model assuming the destruction of the magnetic surface near the separatrix due to non-axisymmetric perturbations. The observed spread of the path of high energy electrons also may be explained by the model.

It is necessary to control the density of the superthermal electrons in the scrape-off layer to reduce heavy impurity contamination caused by the evaporation.

The spread of the flux surfaces near the old separatrix due to non-axisymmetric perturbations has a possibility of a reduction of heat flux density on the neutralizer plate or limiter.

Acknowledgments

Our particular thanks are due to Drs. S. Seki, S. Matsuda, M. Yoshikawa, M. Tanaka and Y. Tanaka for their fruitful discussions. We would like to thank Dr. T. Funahashi, Dr. T. Yamauchi and Mr. K. Kumagai for the electron temperature measurement. We are also grateful to Drs. Y. Obata and S. Mori for their continuous encouragement of our work. The members of operating group of DIVA are gratefully acknowledged for their assistance in the experiment.

The observed width of the movement of the null points is less than 3 mm, which gives only 1.5 mm spread at R = 40 cm. Thus this mechanism seems no to be influential on the spread of the drift surfaces.

The non-axisymmetric perturbations may explain the spread of the path of high energy electrons.

6. Conclusions

Behaviors of superthermal electrons in the scrape-off layer in DIVA are experimentally studied. Superthermal electrons are divided into two groups, that is, high energy electrons (10 keV - 100 keV) and epithermal electrons (150 eV - 500 eV). In the normal discharge, the epithermal electrons play an important role in the heat flux density in the scrape-off layer [13-15]. The loss flux of these electrons is measured and explained by a model assuming the destruction of the magnetic surface near the separatrix due to non-axisymmetric perturbations. The observed spread of the path of high energy electrons also may be explained by the model.

It is necessary to control the density of the superthermal electrons in the scrape-off layer to reduce heavy impurity contamination caused by the evaporation.

The spread of the flux surfaces near the old separatrix due to non-axisymmetric perturbations has a possibility of a reduction of heat flux density on the neutralizer plate or limiter.

Acknowledgments

Our particular thanks are due to Drs. S. Seki, S. Matsuda, M. Yoshikawa, M. Tanaka and Y. Tanaka for their fruitful discussions. We would like to thank Dr. T. Funahashi, Dr. T. Yamauchi and Mr. K. Kumagai for the electron temperature measurement. We are also grateful to Drs. Y. Obata and S. Mori for their continuous encouragement of our work. The members of operating group of DIVA are gratefully acknowledged for their assistance in the experiment.

References

[1] Vlasenkov, V. S., Leonov, V. M., Merezhkin, V. G., Muchvatov, V. S., Nucl. Fusion 13 (1973) 509.

[2] Von Goeler, S., Stodiek, W., Sauthoff, N., Selberg, H., Third International Symposium on Toroidal Plasma Confinement (Garching, 1973) paper B-23.

[3] Spong, D. A., Clarke, J. F., Rome, J. A., Kammash, T., Nucl. Fusion 14 (1974) 397.

[4] Shimomura, Y., Maeda, H., Ohtsuka, H., Kitsunezaki, A., Nagashima, T., Yamamoto, S., Kimura, H., Nagami, M., Ueda, N., Funahashi, A., Matoba, T., Kasai, S., Takeuchi, H., Takahashi, K., Tokutake, T., Anno, K., Arai, T., Phys. Fluids 19 (1976) 1635.

[5] Shimomura, Y., Nagashima, T., Kitsunezaki, A., Maeda, H., Ohtsuka, H., Nagami, M., Tokutake, T., Anno, K., Ohga, T., Arai, T., Funahashi, A., Matoba, T., Kasai, S., Shoji, A., Kawakami, T., Yoshikawa, M., Mori, S., "The First Results on JFT-2a (DIVA)", Japan Atomic Energy Research Institute Report JAERI-M 6102 (1976).

[6] Kimura, H., et al., submitted to Nucl. Fusion.

[7] Lebedev, A. N., JETP 48 (1965) 1393 [Soviet Phys. JETP 21 (1965) 931].

[8] Gibson, A., Phys. Fluids 10 (1967) 1553.

[9] Filonenko, N. N., Sagdeev, R. Z., Zaslavsky, G. M., Nucl. Fusion 7 (1967) 253.

[10] Freis, R. P., Hartman, C. W., Hamzeh, F. M., Lichtenberg, A. J., Nucl. Fusion 13 (1973) 533.

[11] Tomita, Y., Seki, S., Momota, H., J. Phys. Soc. Japan 42 (1977) 687.

[12] Kitsunezaki, A., Maeda, H., Shimomura, Y., Nucl. Fusion 14 (1974) 747.

[13] Maeda, H., Fujisawa, N., Shimomura, Y., Funahashi, A., Ohtsuka, H., Yamamoto, S., Nagami, M., Odazima, K., Kimura, H., Ueda, N., Sengoku, S., Maeno, M., Konoshima, S., Suzuki, N., Hirayama, T., Shimada, M., Yamamoto, T., Kawakami, T., Takahashi, K., Matoba, T., Shoji, A., Kumagai, K., Kasai, S., Takeuchi, H., Yamauchi, T., Sugie, T., Shiho, M., Tanaka, M., Tokutake, T., Anno, K., Arai, T., Hiratsuka, H., Shibata, T., Toyoshima, N., Shiina, T., Isaka, M., Matsuzaki, Y., Tani, T., Kodama, K., Yokokura, K., Sunaoshi, H., Kazawa, M., Hasegawa, K., Kunieda, S., in Plasma Physics and Controlled Nuclear Fusion Research (Proc. 6th Int. Conf. Berchtesgarden, 1976) paper CN-35/A-18.

[14] Maeda, H., Ohtsuka, H., Shimomura, Y., Yamamoto, S., Nagami, M., Kimura, H., Ueda, N., Odajima, K., Sengoku, S., Funahashi, A., Matoba, T., Kasai, S., Sugie, T., Shiho, M., Takeuchi, H., Takahashi, K., Kawakami, K., Shoji, A., Yamauchi, T., Tokutake, T., Anno, K., Arai, T., Hiratsuka, H., Shibata, T., Tanaka, M., Kunieda, S., International Symposium on Plasma wall Intereaction (Jülich, 1976) paper E-537.

[15] Yamamoto, S., Maeda, H., Shimomura, Y., Odajima, K., Nagami, M., Kimura, H., Sengoku, S., Ohtsuka, H., Ueda, N., Funahashi, A., Matoba, T., Takeuchi, H., Takahashi, K., Kasai, S., Sugie, T., Shiho, M., Kawakami, T., Kumagai, K., Yamauchi, T., Shoji, A., Tokutake, T., Anno, K., Arai, T., Shibata, T., Hiratsuka, H., Tanaka, M., Tanaka, Y., Kunieda, S., in Controlled Fusion and Plasma Physics (Proc. 8th Europ. Conf. Prague, 1977) to be published.

Table I. Typical Plasma Parameter in DIVA

	Main Plasma	Scrape-off Layer	
	Center	Near Surface	In Divertor Region
Te [eV]	∿250	30	30
Ti [eV]	85	-	30
n_e [cm^{-3}]	2×10^{13}*	$1 \sim 2 \times 10^{12}$	$1 \sim 2 \times 10^{12}$

* Assuming parabolic profile of electron temperature and density.

Table II. Circulation Number

Initial Point Z_0=0 cm. Φ_0=0	Circulation Number
R_0 = 46.38 cm	∿40
R_0 = 46.46 cm	∿52
R_0 = 46.50 cm	∿26
R_0 = 46.55 cm	∿26
R_0 = 46.62 cm	∿64

Table III. Positions of Critical Drift Surface and Separatrix on the Equatorial Plane

	Region
100 keV	R = (71.02 ∿ 71.03) cm
10 keV	R = (70.05 ∿ 70.06) cm
Separatrix	R = (69.66 ∿ 69.67) cm

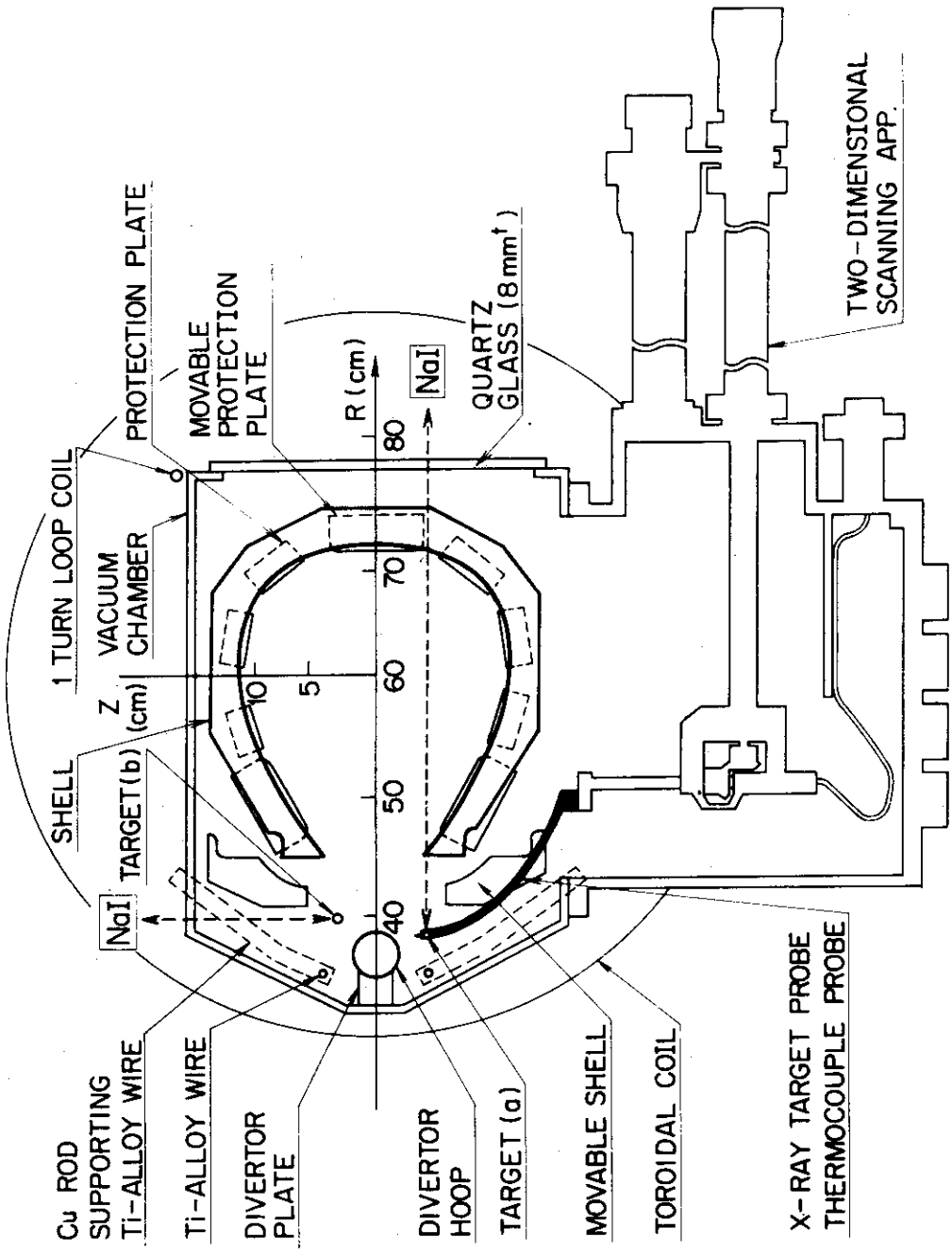

Fig. 1 A schematic diagram of the layout used for the present experiments. X-ray target (a) (4 mm in diameter) is used for the two dimensional measurements of the path of the high energy electrons. X-ray target probe with target (b) (1 mm in diameter) is used for the detailed measurements of spatial distributions of high energy electrons at R = 40 cm.

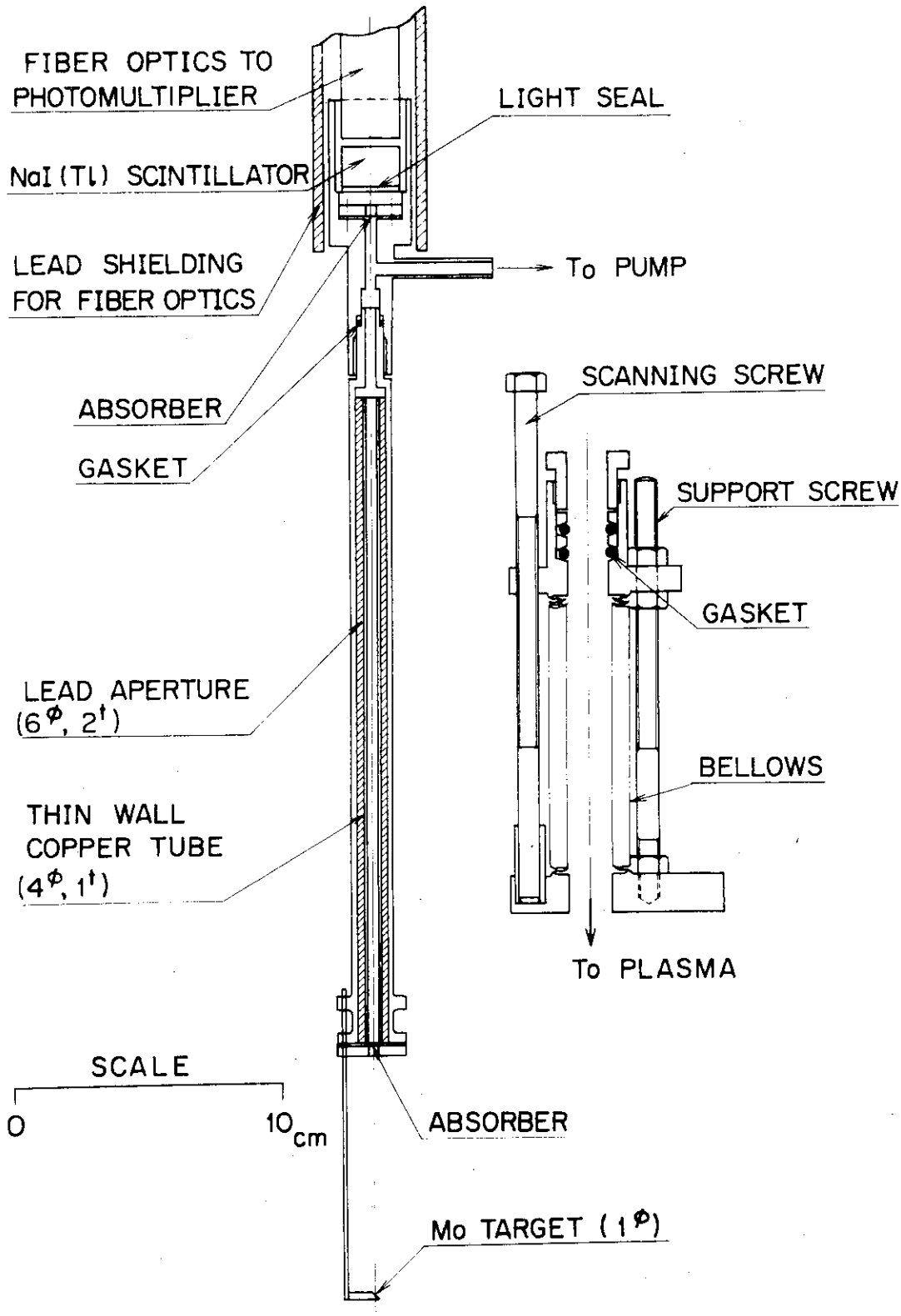

Fig. 2 Side view of X-ray probe with target (b) shown in Fig. 1.

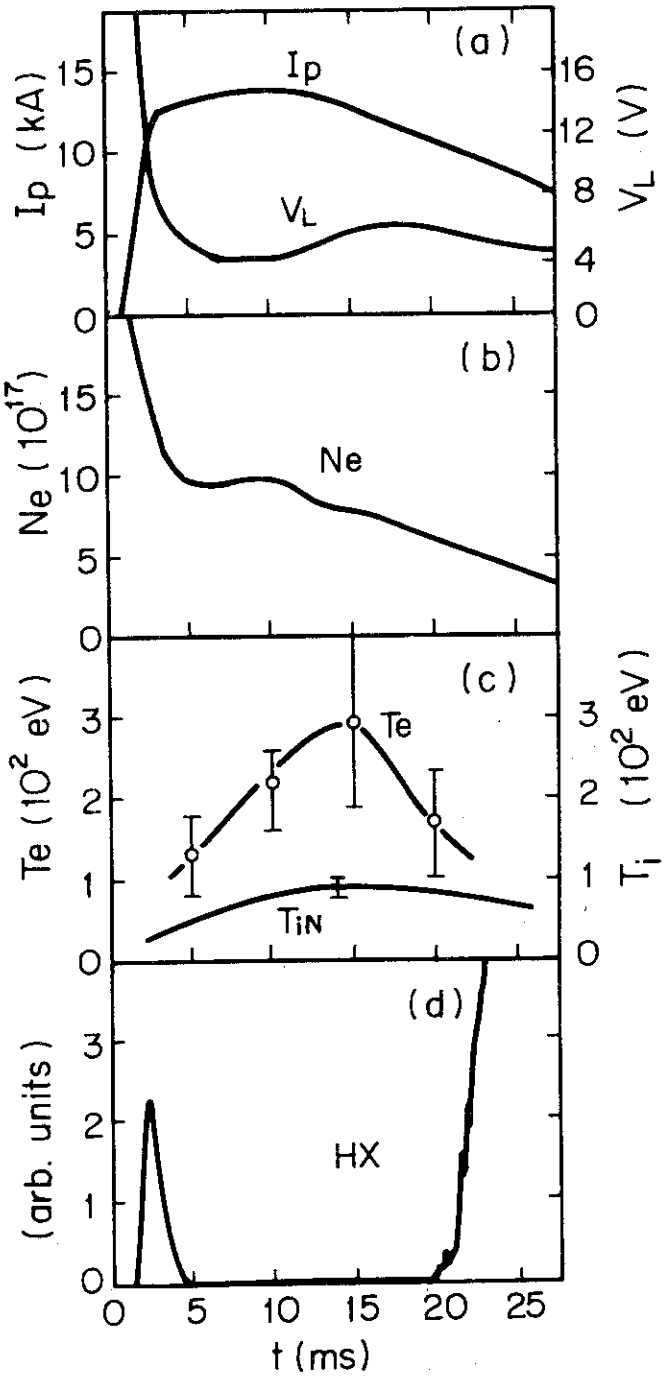

Fig. 3 Time variations of plasma parameters, (a) plasma current, I_p; and loop voltage, V_L; (b) total number of electrons, N_e; and (c) electron temperature, T_e at R = 62 cm and Z = -1 cm, and ion temperature, T_{iN}, obtained by neutral particle energy analysis and (d) hard X-ray radiation.

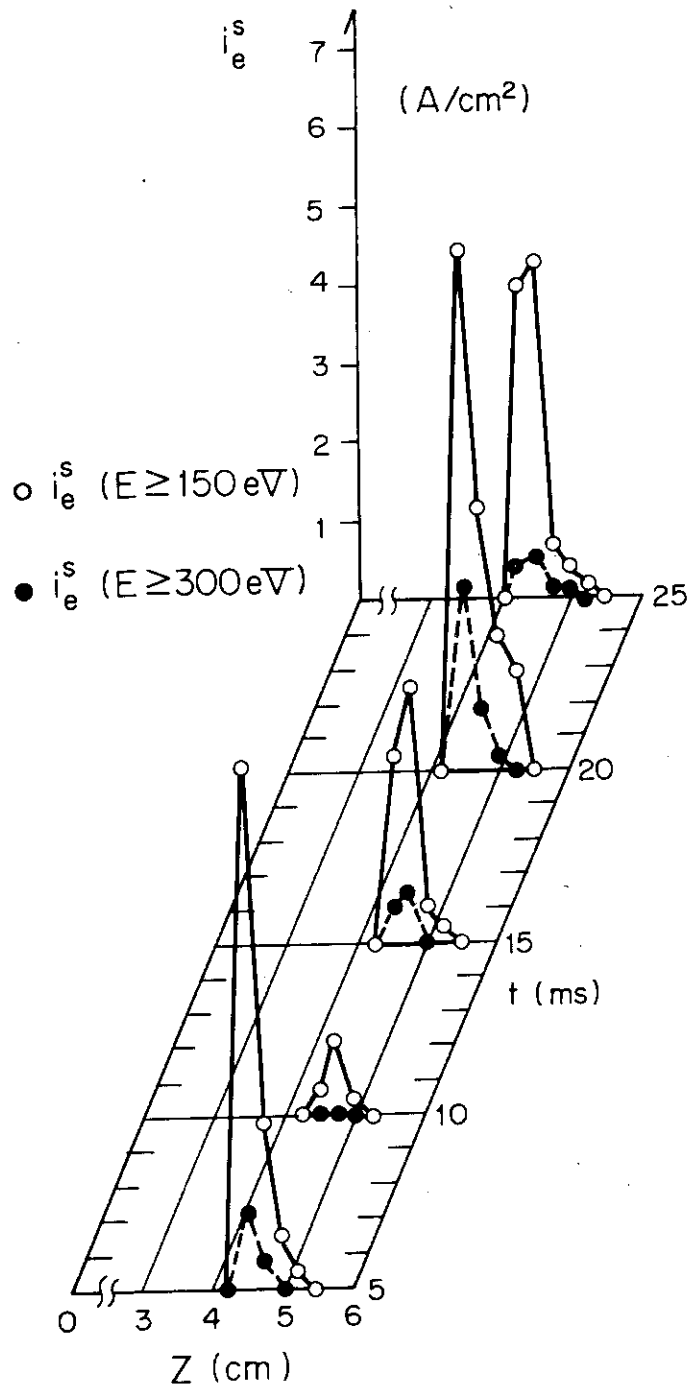

Fig. 4 Vertical profile and time evolution of flux of the epithermal electrons at R = 40 cm. Open circles denote particle fluxes in the energy above 150 eV; and closed circles denote particle fluxes in the energy above 300 eV.

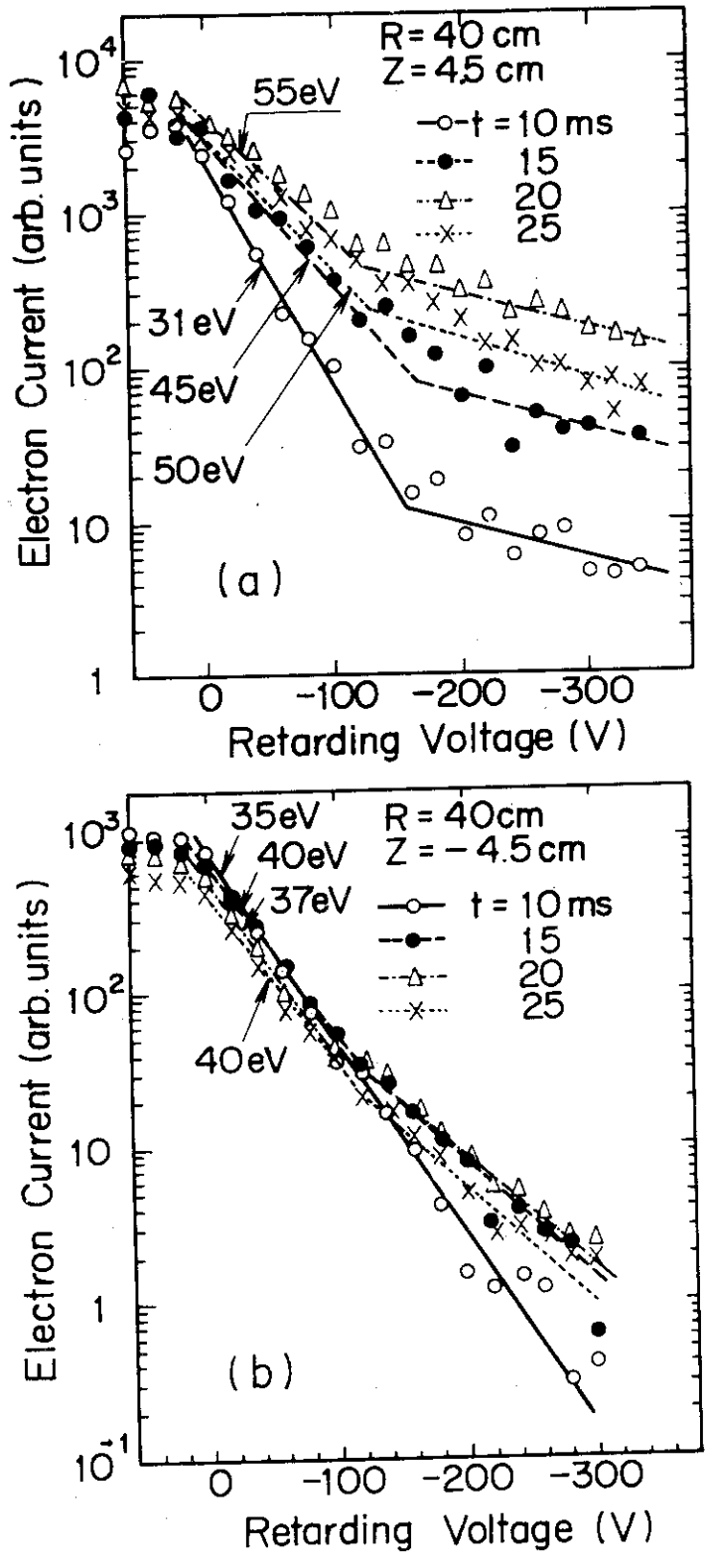

Fig. 5 Energy spectrum of the epithermal electrons at the position R = 40 cm and Z = +4.5 cm (Sub-figure (a)) and at the position R = 40 cm and Z = -4.5 cm (Sub-figure (b)).

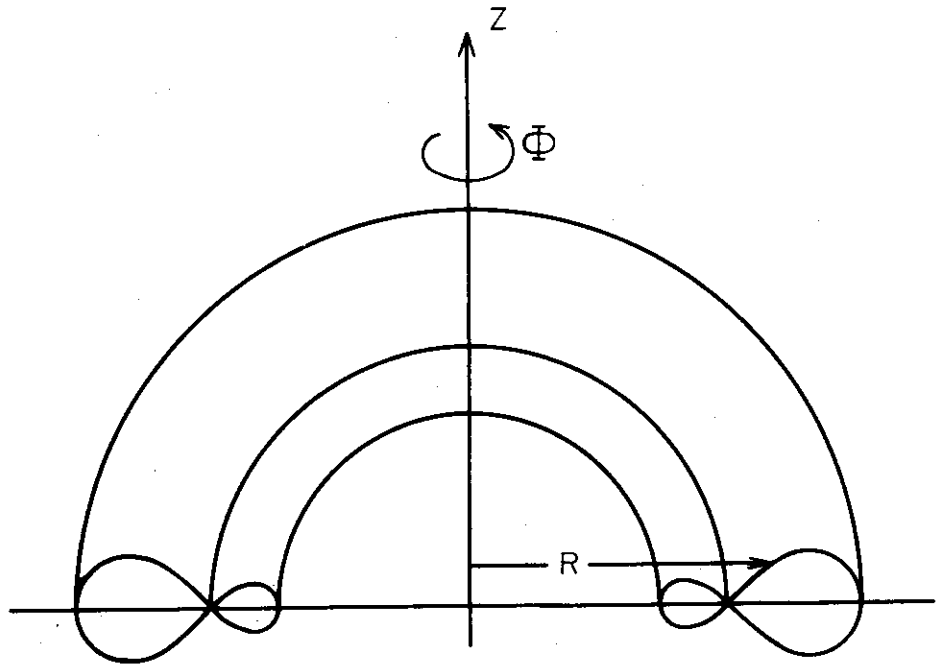

Fig. 6 (R, Φ, Z) co-ordinate system.

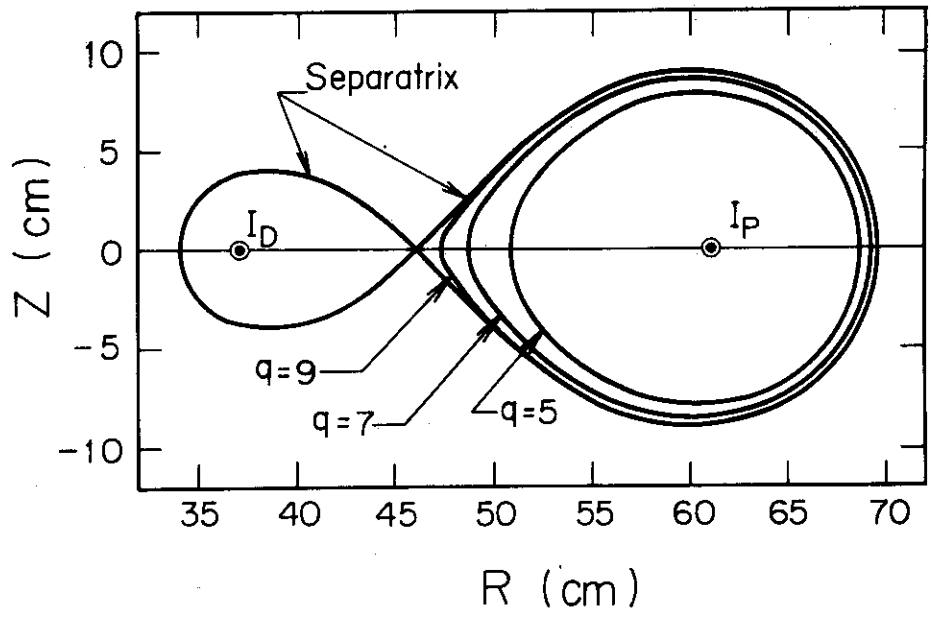

Fig. 7 Unperturbed magnetic surfaces. The rings are located at the positions of R = R_p (R_p = 61 cm) and R = R_D (R_D = 37 cm), respectively. And also shaping coils are located at the positions of R = 110 cm and Z = ±70 cm. The position of the null point is in the region between R = 46.19 cm and R = 46.20 cm on the equatorial plane in the case of I_p = -13.3 kA, I_D = -16 kA and I_s = +8 kA.

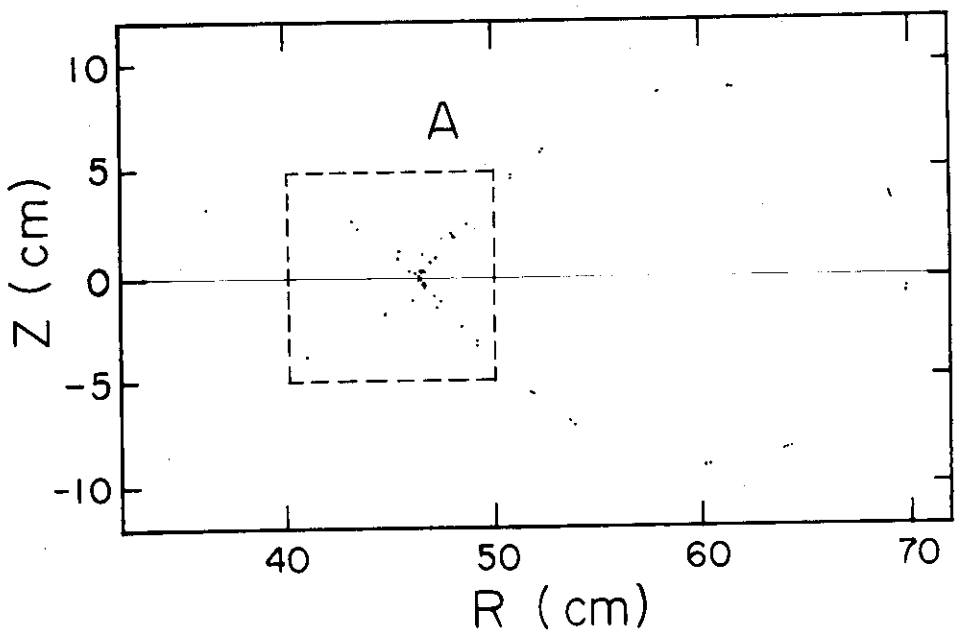

Fig. 8 Behaviors of the field lines near the old separatrix in the case of $\alpha = 10^{-3}$ T and N = 1. The dots in the figure denote the coordinate of the point depicting the field line through each field period with the initial value $R_0 = 46.46$ cm, $Z_0 = 0$ cm and $\Phi_0 = 0$. The region A in this figure is shown expanded in Fig. 9.

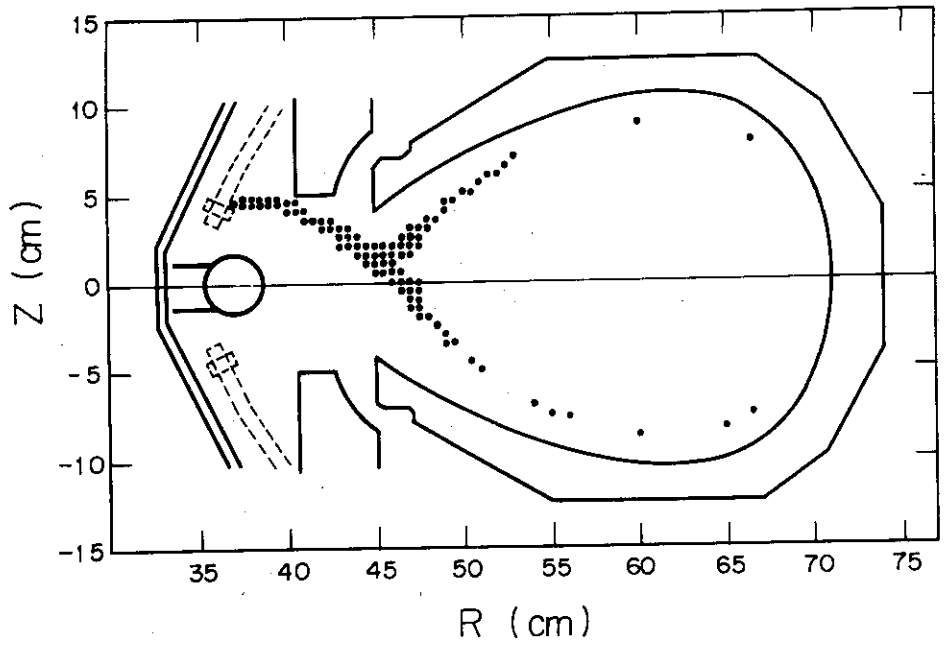

Fig. 10 The path of the high energy electrons (10 keV - 100 keV) at 20 msec.

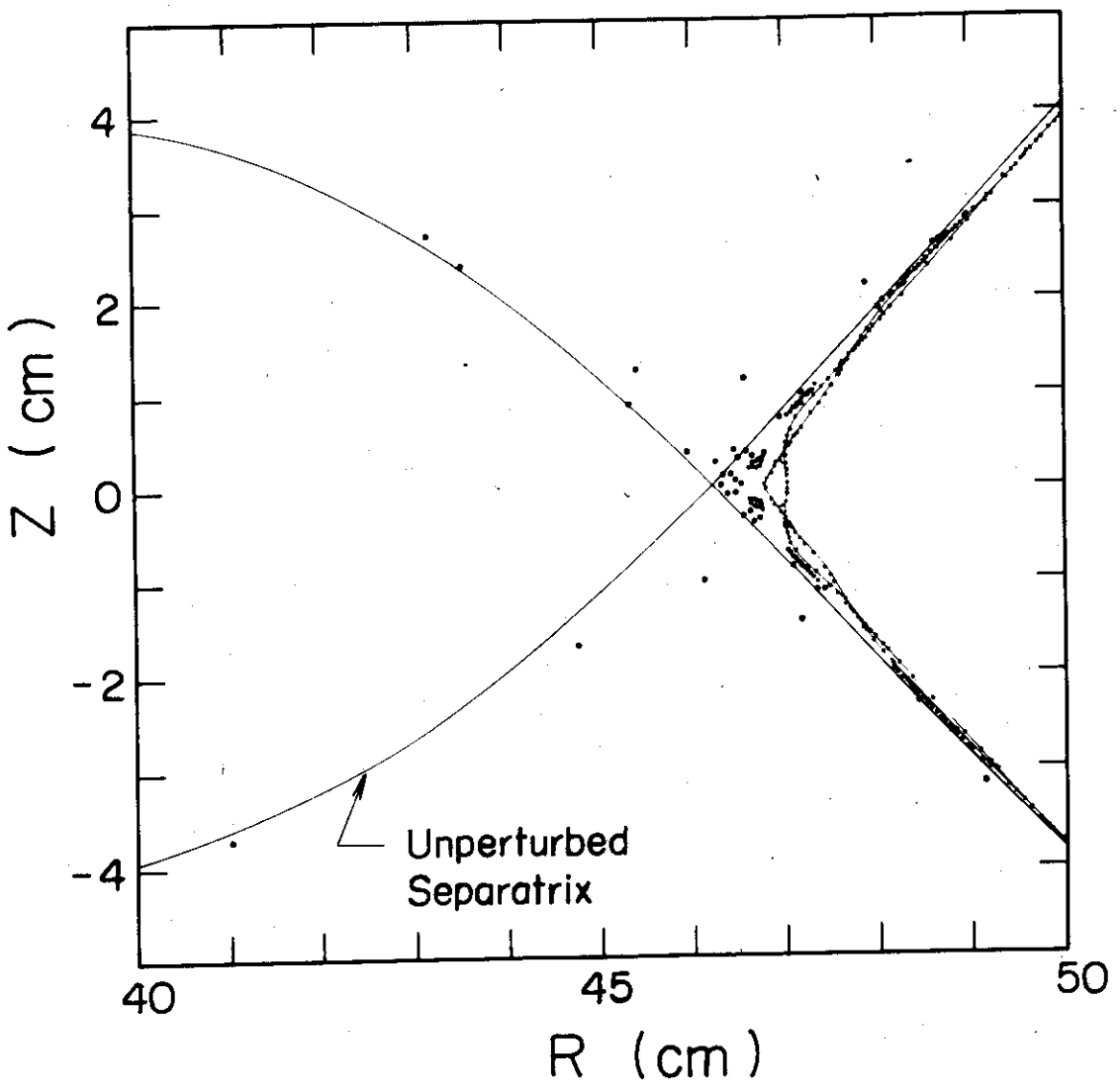

Fig. 9 This figure shows the region A in Fig. 8. The solid line shows the old separatrix. The island structures are observed on the old q = 10 and q = 11 rational surfaces.

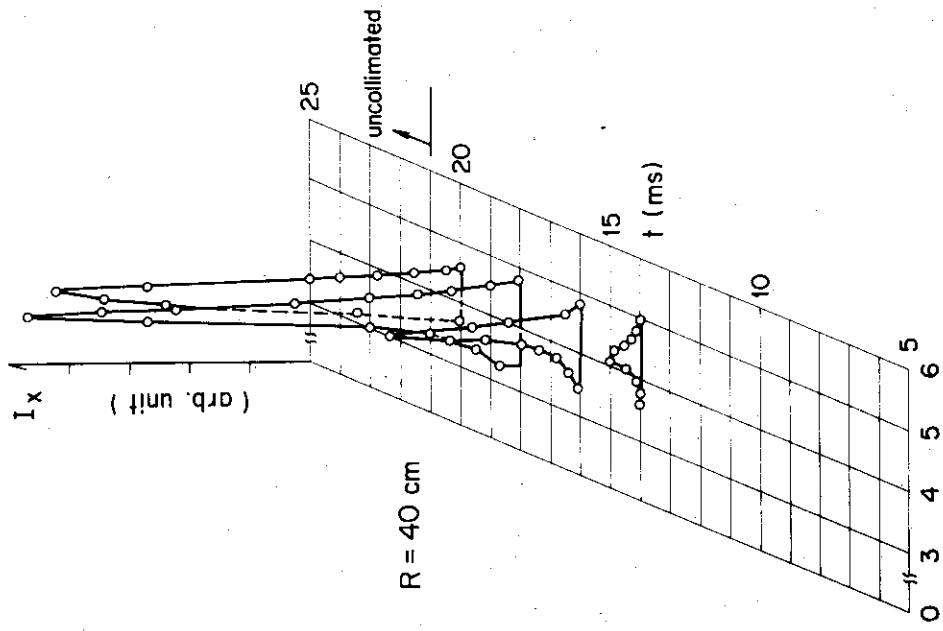

Fig. 12 Vertical profiles and time evolutions of the high energy electrons measured with the target probe with rarget (b) (1 mm in diameter) at R = 40 cm.

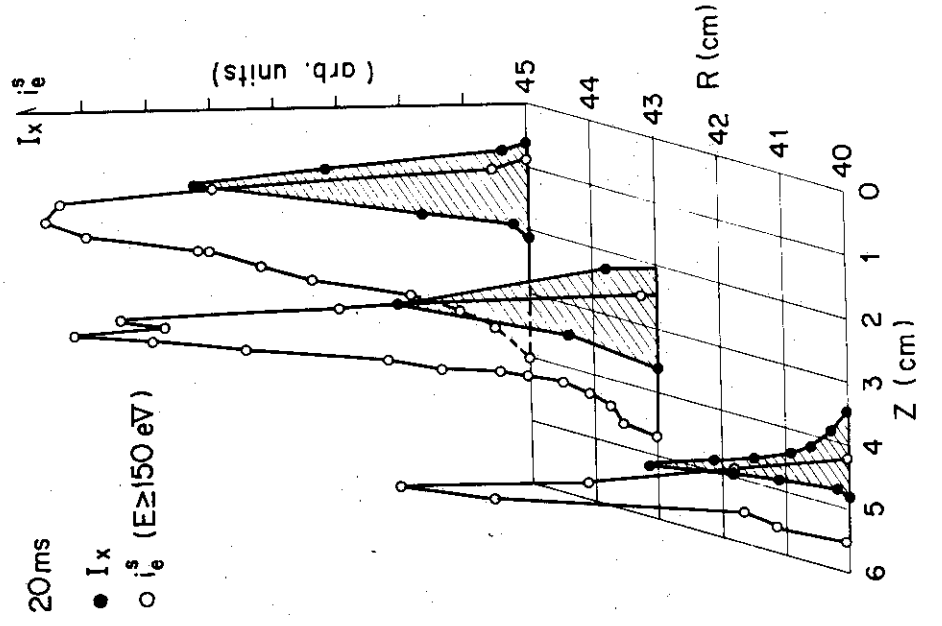

Fig. 11 Vertical profiles of the high energy electrons and particle fluxes of the epithermal electrons in the energy above 150 eV at the positions R = 40, 43 and 45 cm at t = 20 msec.

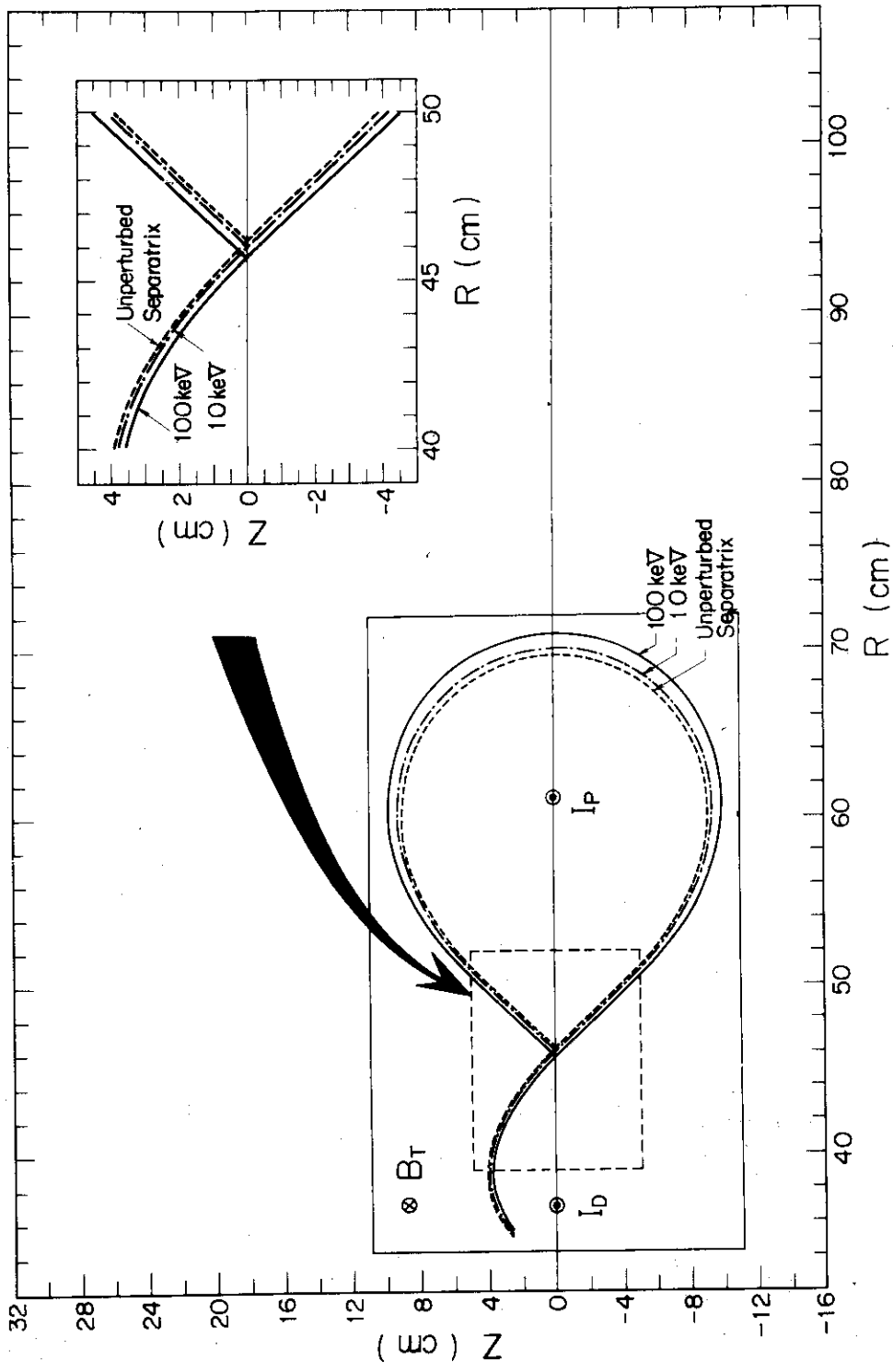

Fig. 13 Drift surfaces of the high energy electrons projected on a minor cross section. The solid lines denote the electron in the energy of 100 keV and the broken line in the energy of 10 keV. The dotted line denotes the separatrix.